

Examination of the influence of several factors on longshore current computation with random waves

Yoshimi Goda

Yokohama National University, Advisor to ECOH CORPORATION, 2-6-4 Kita-Ueno, Taito-Ku, Tokyo 110-0014, Japan

Available online 28 November 2005

Abstract

Influence of various factors affecting the longshore currents induced by obliquely incident random waves is examined through numerical calculation. Seven numerical models for random wave breaking process are found to yield large differences in the wave heights in the surf zone and longshore current velocities. The turbulent eddy viscosity formulation by Larson and Kraus [Larson, M. and Kraus, N.C. (1991): Numerical model of longshore current for bar and trough beaches, *J. Waterway, Port, Coastal, and Ocean Eng.*, ASCE, 117 (4), pp. 326-347.] functions almost equal to that by Battjes [Battjes, J.A. (1975): Modeling of turbulence in the surf zone, *Proc. Symp. Modeling Techniques*, pp. 1050–1061.], but the formulation by Longuet-Higgins [Longuet-Higgins, M.S. (1970): Longshore current generated by obliquely incident sea waves, 1 and 2, *J. Geophys. Res.*, 75 (33), pp. 6779–6801.] produces excessive diffusion of longshore currents into the offshore zone. The generation and decay process of the surface roller is indispensable in the longshore current analysis. The random wave transformation model called PEGBIS (Parabolic Equation with Gradational Breaker Index for Spectral waves) by Goda [Goda, Y. (2004): A 2-D random wave transformation model with gradational breaker index, *Coastal Engineering Journal*, JSCE and World Scientific, 46 (1), pp. 1–38.] produced good agreement with several laboratory and field data of longshore currents.

© 2005 Elsevier B.V. All rights reserved.

1. Introduction

The prediction of longshore currents induced by obliquely incident waves is based on the theory by Longuet-Higgins (1970) with the concept of the radiation stresses. He dealt with the regular waves that break at a fixed location across which the radiation stresses change abruptly. The abrupt change yields a triangular cross-shore profile of longshore velocity, which linearly increases from the shoreline and drops to zero at and beyond the breaker line. To remedy the discontinuity of longshore current velocity across the breaker line, Longuet-Higgins introduced a term of horizontal mixing in the equation of longshore currents.

Waves in the coast are not of regular trains but of random nature. The heights, periods, and directions of individual waves are all different, and their characteristics are best described with the concept of directional wave spectrum. Battjes (1972) was the first in presenting the computation of longshore currents induced by random waves. He clearly showed smooth

variations of longshore current velocity across the surf zone without introducing a horizontal mixing term. Unfortunately, his work did not attract the attention of many researchers who had been accustomed with the regular wave approach. Then, Thornton and Guza (1986) presented a theory of longshore currents for random waves based on their random wave-breaking model in 1983 and showed the theory in good agreement with field measurement data. Goda and Watanabe (1991) also calculated the longshore current velocity on planar beaches with the random wave-breaking model by Goda (1975). They prepared a set of design diagrams for estimation of the cross-shore profiles of longshore currents from the input data of offshore wave heights, periods, and directions. Empirical formulas based on these diagrams are listed in Goda (2000, Sec. 3.9).

The speed and cross-shore profile of longshore currents are governed by the rate of wave energy dissipation. Because each random wave-breaking model produces its own prediction of wave height change in the surf zone, which differs from one model to another, the longshore currents computed by various wave models differ to a large extent. The present paper firstly aims at demonstrating the differences between various random

E-mail address: goda@ecoh.co.jp.

wave-breaking models in both the wave heights and longshore velocities and to call engineers' attention to the importance of selecting a good wave model.

The second purpose of the present paper is to examine the turbulent eddy viscosity formulation and to find out the best one for longshore currents induced by random waves. Although inclusion of the horizontal mixing term is not necessary for planar beaches as demonstrated by Battjes (1974), Thornton and Guza (1986), and Goda and Watanabe (1991), it is indispensable for barred beaches in which the turbulent eddy viscosity helps to diffuse longshore currents over the trough area.

The third objective of the present paper is to clarify the role of surface rollers on generation of longshore currents and to present a workable formulation for the longshore current equation.

Lastly, the new wave transformation model called with an acronymic name of PEGBIS (*Parabolic Equation with Gradational Breaker Index for Spectral waves*) by Goda (2004) is tested for various laboratory and field data to see how well it succeeds in predicting wave heights and longshore current velocities. All the computations presented hereon are limited to beaches of alongshore uniformity (straight, parallel depth contours), but the findings in the present paper will be applicable to nearshore current computations for beaches with arbitrary bathymetry.

2. Random wave-breaking models

2.1. Characteristics of wave models under comparative study

Collins (1970) seems to be the first in presenting a model for wave transformation by random wave breaking. Although the model inspired researchers in developing various wave models to follow, it was not easy to use and has not been employed in practical applications. Among various models so far available, seven models listed in Table 1 are compared for their performance. They have been selected to provide an overview of historical development of random wave breaking models, and it is not intended to cover all the major models.

Wave models examined are those by Battjes (1972), Kuo and Kuo (1974), Goda (1975), Battjes and Janssen (1978), Thornton and Guza (1983), Larson and Kraus (1991), and Goda (2004). All the models define the breaking wave height in terms of water depth, i.e. as a function of H_b/h . The effects

on breaking wave height of wave period expressed as a function of h/L , bottom slope, fluctuation of breaker heights, and wave setup are taken into account by these models, but the degree of inclusion differs among the models as seen in Table 1.

The first two models by Battjes (1972) and Kuo and Kuo (1974) truncate the probability density function (pdf) of wave heights above the breaking wave height. While Battjes' model retains the broken waves at the limiting height with a form of delta function, Kuo and Kuo's model redistributes the portion of broken waves in the range of nonbroken waves by linearly enhancing the remaining pdf. Goda (1975) takes the same approach with that by Kuo and Kuo, but he allows fluctuation of breaker heights over a certain range. His model also includes the effect of bottom slope on the breaking wave height. Like Battjes' model, the breaker height is calculated with the water depth adjusted for the water level change by wave setup.

These three models implicitly estimate the wave energy dissipation from the deformation of pdf. The model by Battjes and Janssen (1978) directly estimates the energy dissipation in analogy to the bore of hydraulic jumps. Formulations of breaker height and pdf are same as Battjes (1972). Thornton and Guza (1983) also employ the concept of bore energy dissipation, but the method of deforming pdf is made by introducing a weighting function for broken waves.

In 1985, Dally et al. proposed a concept of wave energy dissipation, the rate of which is proportional to the difference between the energy flux of waves (under breaking process) and that of stable waves after wave reformation. They applied it for regular waves, but Larson and Kraus (1991) calculated the energy dissipation of individual waves of different height with this concept, thus presenting a random wave-breaking model. This concept is called the Dally model for simplicity.

All the above models represent random waves with a single wave period. However, the model by Goda (2004) fully introduces the directional wave spectrum as the input condition. Some details of this model are discussed in the next subsection.

Random wave breaking models may also be classified into two groups, one for estimation of a single characteristic wave height such as H_{rms} and another for yielding various definitions of wave heights such as H_{max} , $H_{1/20}$, $H_{1/3}$, H_{rms} , etc. The Battjes and Janssen model (1978) is typical of the former, while the Goda models (1975 and 2004) belong to the latter. The models in the former group are cost-effective in CPU time and

Table 1
Main characteristics of random wave-breaking models

Models	Energy dissipation mechanism	PDF of broken waves	Factors affecting breaking wave height					Wave spectrum
			H_b/h	h/L	bottom slope	range allowance	wave setup	
Battjes '72	Pdf deformation	Delta function at breaker height	Yes	Yes	No	No	Yes	No
Kuo and Kuo '74	Ditto	Remove and adjust the remainder	Yes	No	No	No	No	No
Goda '75	Ditto	ditto	Yes	Yes	Yes	Yes	Yes	No
Battjes and Janssen '78	Bore model	Delta function at breaker height	Yes	Yes	No	No	Yes	No
Thornton and Guza '83	Ditto	Adjust with weight function	Yes	No	No	No	No	No
Larson and Kraus '91	Dally model	Delta function at breaker height	Yes	No	No	No	Yes	No
Goda '04 (PEGBIS)	Ditto	Remove and adjust the remainder	Yes	Yes	Yes	Yes	Partially	Yes

are employed in the computation of wave setup and longshore currents, because the information of H_{rms} alone is sufficient for such computations. The models in the latter group are intended to provide the information required for maritime structure designs as well as for the computation of nearshore hydrodynamics. The computational load of these models is not a burden for present-day computers anymore.

2.2. PEGBIS model by Goda (2004)

The new model by Goda (2004) is for two-dimensional wave transformation based on the parabolic equation, which can handle wave shoaling, refraction, and diffraction on arbitrary bathymetry. The basic equation is the one developed by Hirakuchi and Maruyama (1986) for application to oblique wave incidence, which solves the spatial distribution of the steady-state complex velocity potential ϕ based on the following equation:

$$\frac{\partial \phi}{\partial x} = \left\{ i \left(k_x + \frac{k_y^2}{2k_x} \right) - \frac{1}{2k_x c c_g} \frac{\partial}{\partial x} (k_x c c_g) \right\} \phi + \frac{i}{2k_x c c_g} \frac{\partial}{\partial y} \left(c c_g \frac{\partial \phi}{\partial y} \right) - f_D \phi \quad (1)$$

where x and y are the Cartesian coordinates, i denotes the unit imaginary number, k_x and k_y are the wave numbers in the x and y directions, respectively, c denotes the wave celerity, and c_g is the group velocity. The term f_D represents the factor of wave attenuation as below.

The rate of wave attenuation is set as proportional to the complex amplitude of velocity potential as expressed by the last term of Eq. (1). Its coefficient is hereby assumed to comprise of the two components; i.e., f_{Db} for wave breaking and f_{Df} for wave attenuation by bottom friction. Thus,

$$f_D = f_{Db} + f_{Df} \quad (2)$$

The wave attenuation factor by breaking is formulated after the Dally model with some modifications as given by Eq. (3).

$$f_{Db} = \begin{cases} 0 & : a < \gamma h \\ \frac{K_b}{2h} \left[\left(\frac{a}{\gamma h} \right)^2 - 1 \right]^2 & : a \geq \gamma h \end{cases} \quad (3)$$

where h is the water depth before wave actions, a is the wave amplitude, γ denotes the ratio of breaking limit amplitude to water depth, which is called the breaker index in this paper, and K_b is the constant with the value originally set at 0.125. However, Tajima and Madsen (2002) proposed to vary its value with the bottom slope. By adopting their approach, the following empirical formula that gives best fitting to the surf zone wave height curves by Goda (1975) is employed in the present paper:

$$K_b = \frac{3}{8} (0.3 + 2.4s) \quad (4)$$

where s denotes the bottom slope. The slope s is set 0 for the case of $s < 0$.

Wave attenuation by bottom friction is evaluated by calculating the rate of energy dissipation within the turbulent boundary layer due to the shear stress. Calculation yields the following attenuation factor:

$$f_{Df} = \frac{3}{4\pi} C_f \frac{a}{h^2} \frac{k^2 h^2}{\sinh kh (\sinh 2kh + 2kh)} \quad (5)$$

where C_f is the coefficient of bottom friction.

The breaker index γ is not a constant but is given a value gradated with respect to the level of individual wave heights within their distribution. The wave height distribution is assumed as being the Rayleigh distribution, which is divided into M segments with the equal probability of occurrence. The wave height representing each segment is calculated by the following formula:

$$H_m = 0.706 (H_{1/3})_0 \left[\ln \frac{2M}{2m-1} \right]^{1/2} : m = 1, 2, \dots, M \quad (6)$$

where m is the order number descending from the largest one and $(H_{1/3})_0$ denotes the offshore significant wave height.

In order to properly simulate the random wave breaking process, the breaker index is assigned the gradated value of Eq. (7) for each wave height level H_m defined by Eq. (6). The new breaker index is hereby called the gradational breaker index. The wave height H_1 in Eq. (7) is the largest segment height corresponding to $m=1$ in Eq. (6).

$$\gamma_m = \left(C_b \frac{L_0}{h} \left\{ 1 - \exp \left[- \frac{1.5\pi h}{L_0} (1 + 15s^{2.5}) \right] \right\} + \beta_0 \frac{H_m}{h} \left(\frac{H_m}{L_0} \right)^{-0.38} \exp(30s^2) \right) \times \left(\frac{H_m}{H_1} \right)^p \quad (7)$$

The empirical constants C_b , β_0 and p have been given the following values through a trial and error procedure for the area of water depth decreasing in the direction of wave propagation.

$$C_b = 0.080, \beta_0 = 0.016, p = 0.3333 \quad (8)$$

In the area of water depth increasing in the direction of wave propagation, another set of constant values have been assigned as below.

$$C_b' = 0.070, \beta_0' = 0.016, p' = 0.6667. \quad (9)$$

The second term in the right-hand side of Eq. (7) involving the constant β_0 is added to represent the feature of non-zero wave height at the shoreline. With the presence of this term, the effect of wave setup on wave heights in the region near the shoreline is partially simulated.

The constant C_b' has been set at (7/8) C_b . Both constants govern the wave heights within the surf zone. They are so-called free parameters, the values of which can be modified to best fit to the laboratory and/or field wave data. The constant values in Eqs. (8) and (9) have been validated with laboratory data and a set of field observation data with a short wave propagation distance. However, the field data over the propagation distance of several hundred meters

were better fitted with the values of $C_b=0.070$ ($C_b=0.0613$). Depending on the degree of wave attenuation in the surf zone, it is suggested to select an appropriate value among the values of $C_b=0.08, 0.07,$ and 0.06 . It is also necessary to reduce their values slightly when a wave height number M is small.

The input directional wave spectrum is represented with spectral component waves having the equal amount of divided energy. Typically, 40 to 100 component waves are employed in a numerical computation, which is repeated for M levels of wave height; the computations in the present paper have been carried out with $M=61$. For further details of the PEGBIS model, see Goda (2004).

2.3. Mutual comparison of wave heights on planar beaches by various wave models

Seven wave transformation models are compared for their performance in predicting the wave height in the surf zone. Planar beaches with the slope of $s=0.10, 0.05, 0.02,$ and 0.01 are used for a test site. Offshore incident waves with the height $(H_{1/3})_0=2.0$ m, the period $T=8.004$ s, and the incident angle $\theta_0=30^\circ$ are input at the offshore boundary of $h=200$ m. In the PEGBIS model with spectral input, the spectral peak period of $T_p=9.1$ s is used.

The formulation of wave breaking limit differs among wave models. Some explanation is given before presenting the results of wave height computation. Battjes model (1972) and

Battjes and Janssen model (1978) employ the following formula:

$$\frac{H_b}{d} = \frac{0.88}{kd} \tanh\left[\frac{\gamma}{0.88} kd\right] \tag{10}$$

where d denotes the wave height adjusted with the mean water level change by wave setup and the breaker index γ is given a value 0.80 in Battjes model (1972). Although the same value was proposed in Battjes and Janssen model (1978), a more common formula of the following by Battjes and Stive (1985) is used here:

$$\gamma = 0.5 + 0.4 \tanh(33H_{0,rms}/L_{0,p}) \tag{11}$$

Eq. (11) gives the value of $\gamma=0.674$ for the current wave condition.

Among the models not considering the effect of wave period on breaker height, Kuo and Kuo model (1974) uses the formula of $H_b=0.63h$, Thornton and Guza model (1983) uses $(H_{rms})_b=0.42h$, and Larson and Kraus model (1991) employs $H_b=0.78d$. The computed results of wave height variations in the surf zone for four planar beaches are shown in Fig. 1.

Battjes model (1972) and Kuo and Kuo model (1974) yields the wave heights unaffected by the bottom slope. Because other five models produce different wave heights depending on the bottom slopes, the first two models serve as the guide marks for the other models. Although Battjes and Janssen model (1978), Thornton and Guza model (1983), and Larson and Kraus model (1991) do not include the bottom slope effect on the

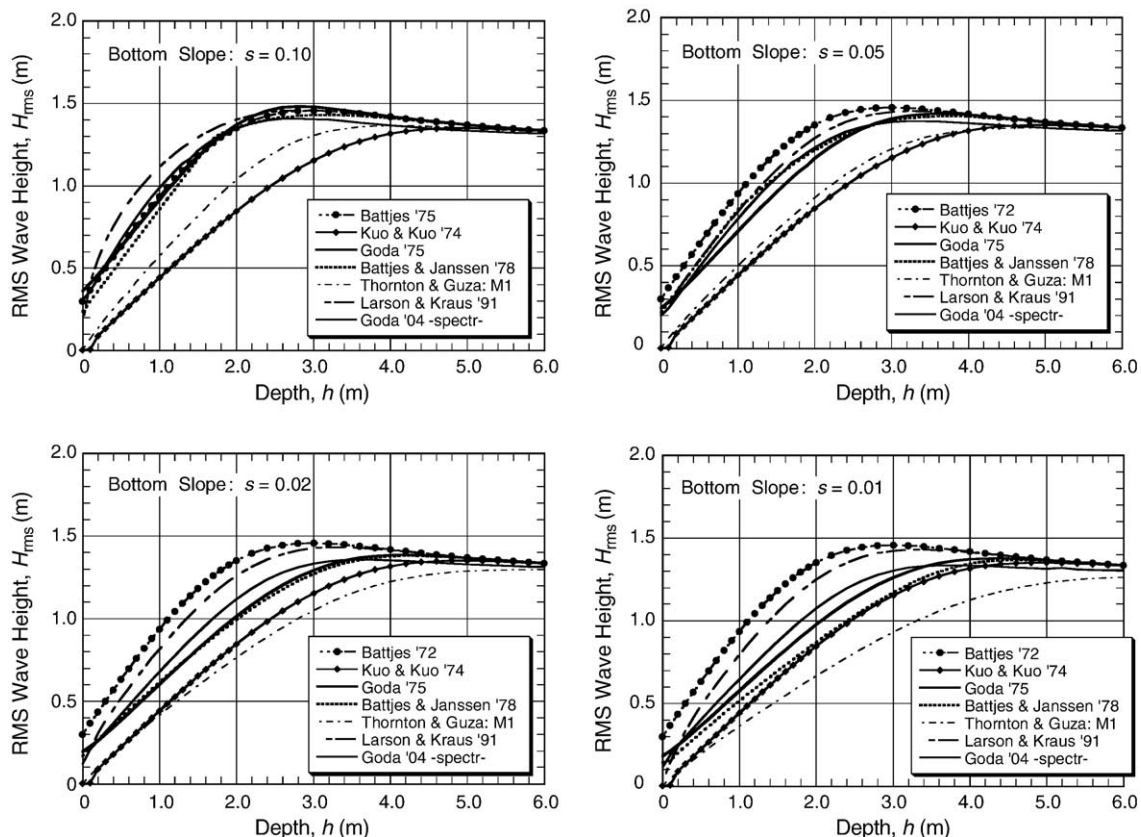


Fig. 1. Wave height variations in the surf zone on planar beaches computed by seven random wave-breaking models for $(H_{1/3})_0=2.0$ m, $T=8.004$ s, and $\theta_0=30^\circ$.

breaker index, they all yield larger wave heights on steep beaches than on mild beaches. Because the process of wave energy dissipation requires a certain distance of wave propagation according to the bore theory or the Dally model, waves on a steep beach cannot have a sufficient distance for full energy dissipation to take place and so they maintain larger heights than waves on a mild beach.

Among the seven models, Larson and Kraus model (1991) and Battjes model (1972) provide larger wave heights than other models. Kuo and Kuo model (1974) and Thornton and Guza model (1983) provide smaller wave heights than other models. Goda model (1975), Battjes and Janssen model (1978), and the PEGBIS model by Goda (2004) provide nearly same heights for the wave conditions tested here.

As demonstrated in Fig. 1, the differences in wave heights between wave transformation models are quite significant. Smith (2001) has also compared several wave models applied for the Duck94 wave data and found large differences. Because of such large differences, one should be careful in selecting a random wave-breaking model for his engineering application.

A shortcoming of Battjes and Janssen model (1978) for application to longshore current computation is that the model produces a discontinuity in the derivative dH/dx owing to an artificial ceiling of $H_{rms}=H_b$ under a certain condition for prevention of unnatural situation of $H_{rms}>H_b$. Fig. 2 shows the wave height variations predicted by this model for four planar beaches. For the slope of $s=0.10$, the discontinuity of dH/dx occurs at the depth $h=1.72$ m, while it occurs at $h=1.02$ m for $s=0.05$; the slopes of $s=0.02$ and 0.01 do not produce such a discontinuity. The location of discontinuity is a function of incident wave steepness, bottom slope, and incident wave angle. An example of diagrams indicating the location of discontinuity has been prepared as shown in Fig. 3, which is the case of normal incidence. The smaller the wave steepness and the steeper the bottom slope, the location of discontinuity appears further offshore.

It should be mentioned here that Baldock et al. (1998) have reformulated the Battjes and Janssen model (1978) by abandoning the depth limitation of $H_{rms}=H_b$ and employing a standard Rayleigh pdf for evaluation of wave energy dissipation. The model does not produce the discontinuity of

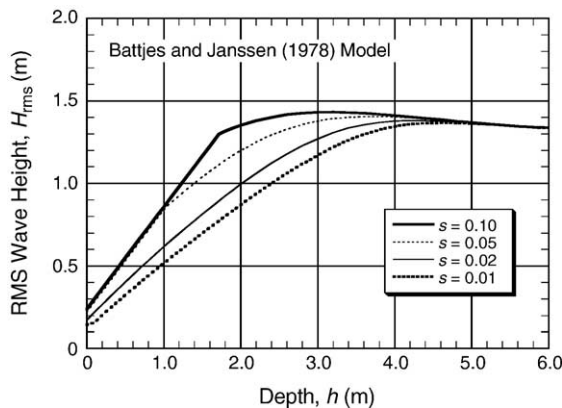


Fig. 2. Wave height variation by Battjes and Janssen model for incident angle of $\theta_0=30^\circ$.

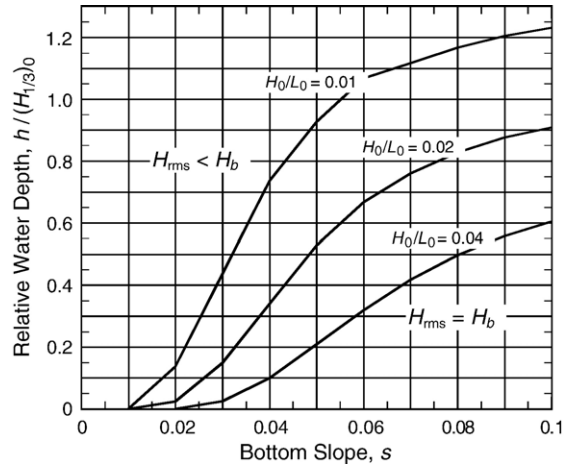


Fig. 3. Location of the discontinuity of dH/dx for $\theta_0=0^\circ$.

dH/dx . They have reported good results for the cross-shore variation in both wave height and the fraction of broken waves on laboratory beaches.

3. Comparison of turbulent eddy viscosity formulations

The theory of longshore currents by Longuet-Higgins (1970) states that the driving force of the radiation stress gradient dS_{xy}/dx is balanced with the bottom shear stress F_y and the resultant longshore currents are smoothed out through the horizontal mixing. The governing equation for the longshore current velocity V is thus expressed as

$$\frac{dS_{xy}}{dx} - \frac{d}{dx} \left(\rho v h \frac{dV}{dx} \right) + F_y = 0 \quad (12)$$

The second term is for horizontal mixing with ρ being the density of water and v being the turbulent eddy viscosity. For the time-averaged bottom shear stress \bar{F}_y , Longuet-Higgins gave a linear approximation of the following under the condition that the longshore current velocity V is much slower than the maximum orbital velocity u_{max} of water particles at the bottom:

$$\bar{F}_y = \frac{2}{\pi} \rho C_f u_{max} V \quad (13)$$

Although there have been much arguments on the validity of the linear approximation, this formula is employed in the present paper with u_{max} being evaluated for the root-mean-square wave height of random waves. It is because other factors, such as the selection of a wave model, evaluation of eddy viscosity, inclusion of surface rollers etc., exercise far greater influence on the prediction of longshore current velocity than the formulation of bottom shear stress.

Longuet-Higgins argued that the turbulent eddy viscosity should be a product of representative length and velocity and proposed the following formula:

$$v = N|x|(gh)^{1/2} \quad (14)$$

where x is the distance from the shoreline and N is a constant in the range of 0 to 0.016. The formula works well when applied

for longshore currents induced by regular waves. However, Thornton and Guza (1986) already pointed out that their theory of longshore currents induced by random waves could perform well without the term of horizontal mixing, because the radiation stress S_{xy} of random waves varies smoothly within the surf zone in contrast to the abrupt change of S_{xy} across the breaking line in case of regular waves.

Battjes (1975) proposed another formula of the turbulent eddy viscosity through scaling arguments that the intensity of turbulence should be related with the rate of wave energy dissipation D per unit area as in the following:

$$v = Mh \left(\frac{D}{\rho} \right)^{1/3} \tag{15}$$

where M is a constant in the order of 1. This formula is employed by a number of researchers since then.

Another formula has also been proposed by Larson and Kraus (1991) with the intention of preventing dispersion of longshore currents outside the surf zone, by making the turbulent eddy viscosity decrease rapidly in deepwater. The formula employs the wave height H and the maximum orbital velocity u_{max} at the bottom as representative of length and velocity, respectively. It is expressed as

$$v = Au_{max}H \tag{16}$$

where A is a constant having a value around 0.3 to 0.5.

Effect of the turbulent eddy viscosity on longshore currents depends on the cross-shore distribution of the radiation stress and the resultant cross-shore profiles of longshore currents. Thus, the eddy viscosity effect is influenced by the random wave-breaking model being employed. Performance of the formulas by Longuet-Higgins (Eq. (14)) and Battjes (Eq. (15)) is compared for a planar beach with the slope of $s=0.05$, when random wave breaking is evaluated by Goda model (1975). The incident wave conditions are the same as those for Fig. 1. The left diagram in Fig. 4 employs the eddy viscosity formula of Eq. (14), while the right diagram uses the formulation of Eq.

(15). The ordinate on the left-hand side indicates the longshore current velocity, while that on the right-hand side represents the cross-shore derivative of radiation stress ΔS_{xy} , as measured with the difference of the values of radiation stress between the neighboring grids in arbitrary units to indicate the variation of current driving force.

The formula for turbulent eddy viscosity by Longuet-Higgins (1970) produces excessive dispersion of longshore currents in the region deeper than 5 m even when the constant N is as small as 0.001. The formula by Battjes (1975) does not produce large dispersion of longshore currents as compared with the one by Longuet-Higgins (1970), but the constant M is hereby recommended to be given a value less than around 0.5 so as to limit a decrease of peak velocity.

Another test is made for the performance of the turbulent eddy viscosity formulas for the case when random wave breaking is evaluated by Battjes and Janssen model (1978). Fig. 5 shows comparison of the performance of the eddy viscosity formulas by Battjes (1975) and Larson and Kraus (1991) for smoothing the cross-shore profile of longshore currents.

For this wave condition, the gradient of radiation stress abruptly changes at the depth of about 1.02 m owing to the limitation of $H_{rms}=H_b$, as discussed in Figs. 2 and 3. The longshore current velocity also jumps at this location without horizontal mixing, but the sudden change is smoothed out as the value of constant M or A is raised and the degree of horizontal mixing is intensified.

The formula for turbulent eddy viscosity by Battjes (1975) produces dispersion of longshore currents in the region deeper than 5 m, which is outside the surf zone, if the constant M is given a large value, say 1.0. In the region deeper than 5 m, there exists a minute but finite amount of the energy dissipation rate D , and the turbulent eddy viscosity maintains a certain magnitude because it is the product of the water depth and the one-third power of energy dissipation rate.

The formula by Larson and Kraus (1991) produces almost the same magnitude of dispersion of longshore currents in

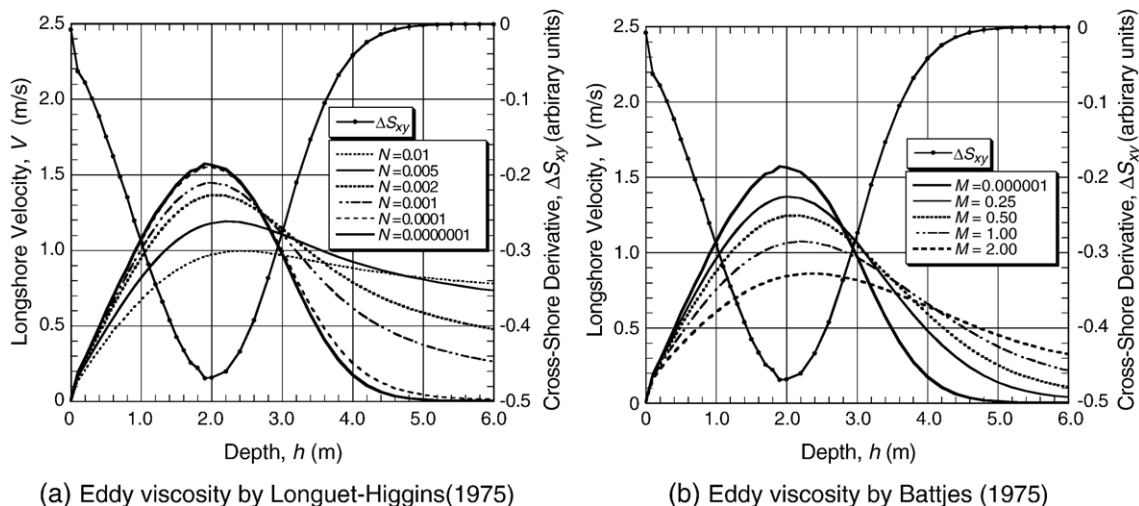


Fig. 4. Cross-shore variation of longshore current velocity evaluated with Goda model (1975) on planar beach of $s=0.05$ for $(H_{1/3})_0=2.0$ m, $T=8.004$ s, and $\theta_0=30^\circ$.

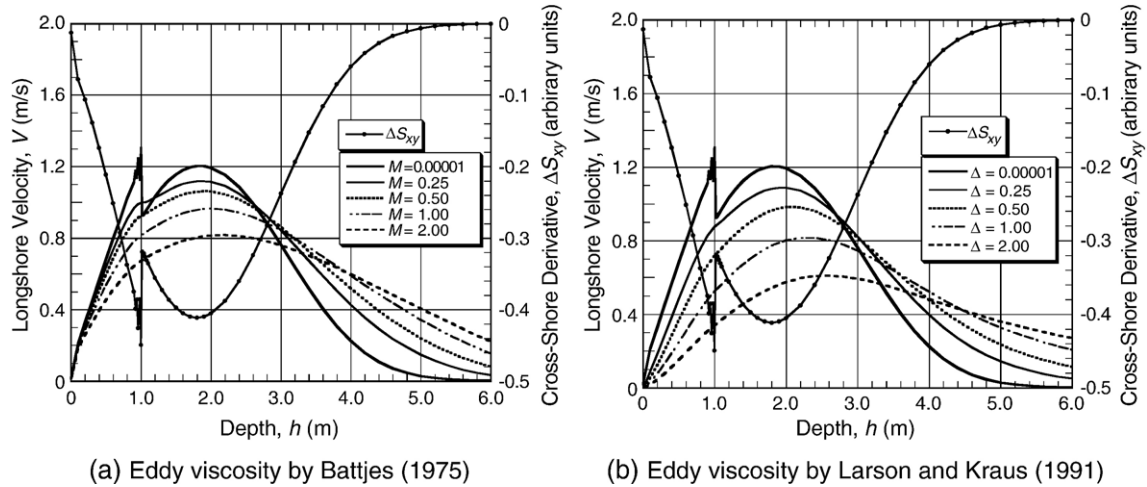


Fig. 5. Cross-shore variation of longshore current velocity evaluated with Battjes and Janssen model (1978) on planar beach of $s=0.05$ for $(H_{1/3})_0=2.0$ m, $T=8.004$ s, and $\theta_0=30^\circ$.

deeper water, but it yields some decrease in the longshore current velocity near the shoreline. The latter feature is a disadvantage of using Eq. (16). However, the formula by Larson and Kraus (1991) is easy to use even in the region behind an offshore breakwater where estimation of wave energy dissipation rate is rather difficult. Therefore, Eq. (16) by Larson and Kraus (1991) can be useful for practical applications, even though it does not have the background of physical

reasoning. In the present paper, the formulation of Eq. (16) is employed for the sake of simplicity.

4. Comparison of longshore currents on planar beaches predicted by various wave models

Large differences in prediction of wave heights between various random wave-breaking models (Fig. 1) imply their

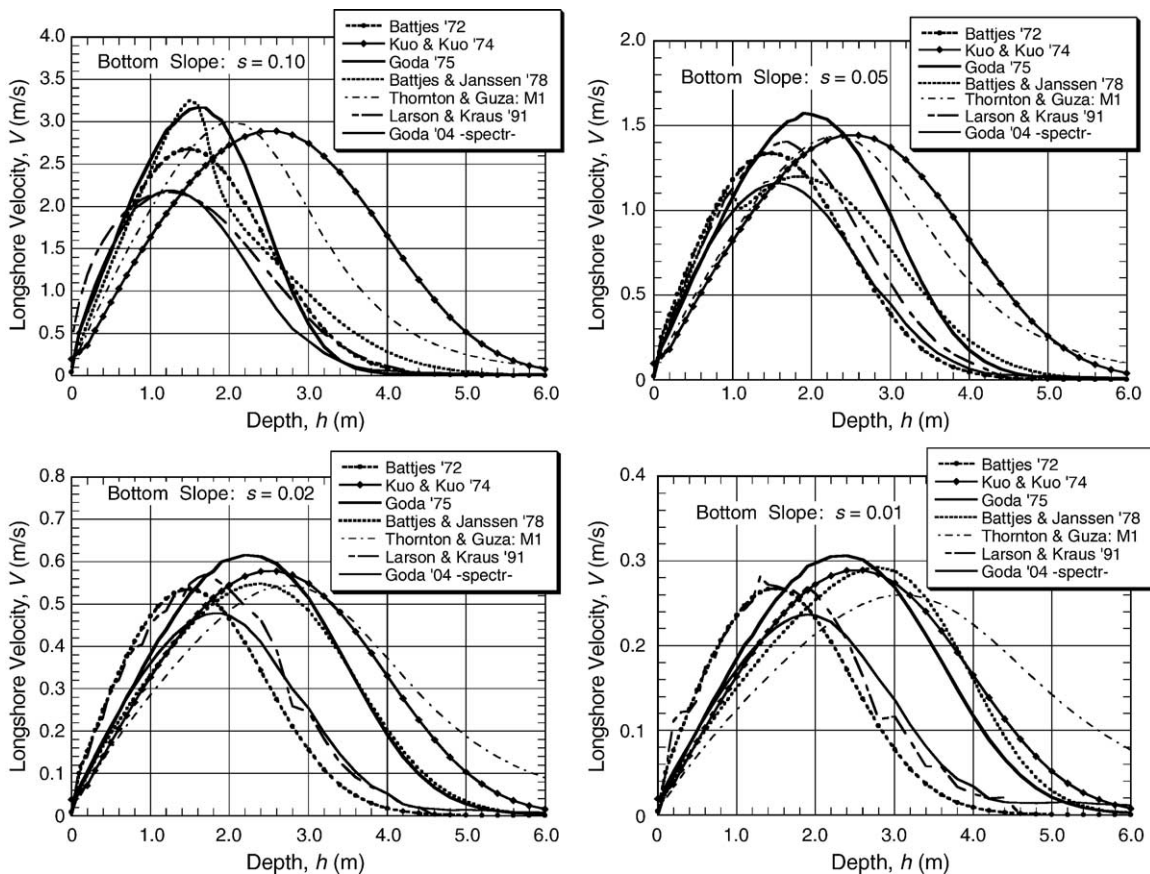


Fig. 6. Longshore current velocity across the surf zone on planar beaches computed by seven random wave-breaking models for $(H_{1/3})_0=2.0$ m, $T=8.004$ s, and $\theta_0=30^\circ$.

diverse performance in prediction of longshore current velocities. Fig. 6 is an example of comparing such performance on planar beaches with the bottom slopes of $s=0.10, 0.05, 0.02,$ and 0.01 . The input wave conditions are the same as those for Fig. 1. In the computation, the turbulent eddy viscosity formula of Eq. (16) is used with the constant value of $A=0.25$ except for the PEGBIS model for which $A=0.1E-4$ is employed. The coefficient of bottom friction is assigned the value of $C_f=0.01$.

Battjes model (1972) and Kuo and Kuo model (1974) are not affected by the bottom slope, and therefore their profiles on different bottom slopes are all similar. The locations of the peak velocity are the same, but its speed decreases in proportion to the bottom inclination. The maximum speeds of longshore currents predicted by the seven wave models do not vary much: differences are at most 30%. However, the locations of peak currents are very different, depending on the wave model employed. Largest differences are observed in the outer part of the surf zone, where some models predict nearly null velocity while other models yield the velocity more than half the peak velocity.

There is no theoretical way to judge the validity of these wave models with regard to longshore current prediction. Only criterion for judgment will be their performance in bringing their prediction in agreement with many data sets of laboratory tests and field measurements. In the sections to follow, the performance of the PEGBIS model by Goda (2004) will be examined, while the examination of the other models is left to the original modelers.

5. Incorporation of surface rollers in longshore current computation

The concept of surface rollers was introduced by Svendsen (1984a,b) for better modeling of wave setup, undertow and others. Surface rollers have since attracted attention of researchers for longshore current modeling, because of their role in shifting the location of the maximum currents toward the shore. On barred beaches, field measurements show the maximum currents appearing not on the top of bars but rather on the troughs shoreward of the bars, as found during DELILAH project (Smith et al., 1992) and at the HORS (Hazaki Oceanographical Research Station) in Ibaraki Prefecture, Japan (Kuriyama and Ozaki, 1993).

According to Svendsen (1984a), the kinetic energy of surface roller averaged over a wave period is given by

$$E_{sr} = \frac{\rho A_{sr} c}{2T} \quad (17)$$

where A_{sr} denotes the area of a surface roller. As a wave begins to break, a zone of white foams is created in the wave front and the water in this zone is actively rotated, thus giving the name of surface rollers. At the point of incipient wave breaking, the surface roller is just born and its area increases as the breaking-to-broken wave propagates. As the height of broken wave gradually decreases through dissipation of wave energy, the surface roller also becomes small and finally disappears; it is a

process of wave reformation to a stabilized state. Thus, the surface roller grows by absorbing a part of wave energy dissipated by wave breaking and then wanes by losing its own energy. Tajima and Madsen (2003) expressed this process as in the following, by referring to the formulation by Dally and Brown (1995):

$$\alpha \nabla (E c_g \vec{n}) + \nabla (E_{sr} c \vec{n}) = - \frac{K_{sr}}{h} E_{sr} c \quad (18)$$

where α is the energy transfer factor taking a value between 0 and 1, $\vec{n} = (\cos\theta, \sin\theta)$ represents the wave direction vector, and K_{sr} represents the dissipation rate of surface roller energy: K_{sr} is taken as equal to K_b of Eq. (4), following the approach of Tajima and Madsen (2003).

The first term in the left-hand side of Eq. (18) represents the rate of energy transfer to the surface roller energy from the dissipated wave energy flux, which is evaluated by a random wave-breaking model independent of surface rollers. For a beach having uniformity in the alongshore direction, Eq. (18) can be rewritten for the surface roller area A_{sr} as in the following:

$$\begin{aligned} \alpha \frac{\partial}{\partial x} \left(\frac{1}{8} \rho g H^2 c_g \cos\theta \right) + \frac{\partial}{\partial x} \left(\frac{\rho A_{sr}}{2T} c^2 \cos\theta \right) \\ = - \frac{K_{sr}}{h} \frac{\rho A_{sr}}{2T} c^2 \end{aligned} \quad (19)$$

By solving Eq. (19) step by step from the offshore to the shoreline with the boundary condition of $A_{sr}=0$, the cross-shore variation of A_{sr} is obtained. In numerical computation for random waves, the root-mean-square wave height H_{rms} is used as H and the mean wave direction as θ in Eq. (19). With A_{sr} having been solved, the cross-shore variation of the surface roller energy E_{sr} is calculated by Eq. (17). The equations for the mean wave level change and the longshore current velocity are modified with incorporation of the surface roller terms as in the following:

$$\frac{\partial \bar{\eta}}{\partial x} = - \frac{1}{(h + \bar{\eta})} \left[\frac{\partial S_{xx}}{\partial x} + \frac{\partial}{\partial x} (2E_{sr} \cos^2\theta) \right] \quad (20)$$

$$\frac{\partial S_{xy}}{\partial x} + \frac{\partial}{\partial x} (E_{sr} \sin 2\theta) - \frac{\partial}{\partial x} \left(\rho v_t h \frac{\partial V}{\partial x} \right) + F_y = 0 \quad (21)$$

The second term in the left-hand side of Eq. (21) is the same as that given by Ruessink et al. (2001).

The wave setup and longshore current velocity are computed with the wave transformation model PEGBIS for waves with the height $(H_{1/3})_0=2.0$ m, the period $T_p=9.1$ s, and the offshore angle $\theta_0=30^\circ$ incident on a planar beach with the slope $s=0.05$. The energy transfer factor from waves to surface rollers is set at several values varying from zero to $\alpha=0.5$. The result of computation is shown in Fig. 7. As the factor of surface roller energy transfer increases, the zone of wave set-down expands toward the shoreline and the wave setup is confined in a narrow region with a sharp rate of increase. As the result, the amount of wave setup at the shoreline increases with the increase of the surface roller energy transfer factor.

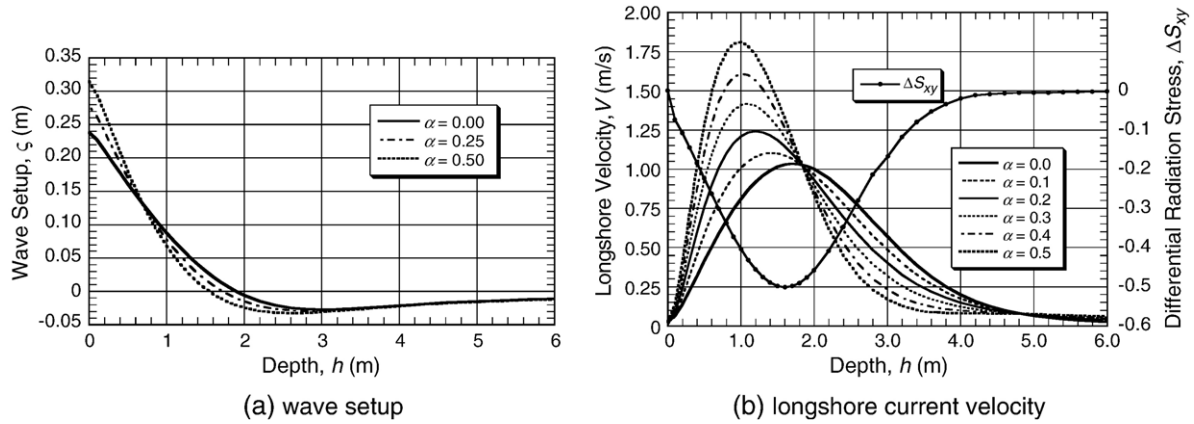


Fig. 7. Variation of wave setup and longshore current velocity by gradual incorporation of surface rollers expressed by the energy transfer factor α for waves incident on a planar beach with $s=0.05$ for $(H_{1/3})_0=2.0$ m, $T_p=9.1$ s, and $\theta_0=30^\circ$.

The longshore current computed by the PEGBIS model maintains a small but finite velocity in the region beyond the depth 5 m, which is induced by wave attenuation by the bottom friction incorporated in the PEGBIS model.

As the surface roller energy transfer factor increases, the peak of longshore current velocity also shifts toward the shoreline with an increase in the maximum velocity. At the initial stage of wave dissipation by breaking, the surface roller area continues to increase and the second term in the left-hand side of Eq. (21) has a positive value and offsets a negative value of the first term, thus delaying the increase of longshore currents. Only after the surface roller area begins to decrease (or the second term takes a negative value), longshore currents shows marked increase of their velocity. The variation of longshore current velocity with respect to the energy transfer factor α shown in Fig. 7 (b) seems to suggest that the value $\alpha=0.5$ is an upper limit and a further raising would cause excessive distortion of longshore current profiles. In fact, Tajima and Madsen (2003) recommend the value $\alpha=0.5$, saying that ‘the surface roller is located above the water surface where potential wave energy resides, whereas most of the kinetic wave energy is distributed over the entire depth and not readily supplied to the surface roller energy’.

6. Comparison of predictions by PEGBIS model and laboratory data

There are not many data sets of random wave tests on longshore current velocity, which could be used for calibration of wave models. In the following, two data sets on fixed beds and two other data sets on movable beds are utilized. The first laboratory data is due to Hamilton and Ebersole (2001), who measured longshore currents induced by unidirectional random waves in the Large-scale Sediment Transport Facility (LSTF) at Coastal and Hydraulics Laboratory, US Army Engineer Research and Development Center, Vicksburg. A uniform slope with $s=1/30$ was built with concrete, and a multiple pump-and-piping system supported circulation of longshore currents in a wave basin. The incident waves of $H_{m0}=0.225$ m,

$T_p=2.5$ s, and $\theta=10^\circ$ were generated in the section of uniform depth of $h=0.667$ m.

Wave heights and longshore currents were computed using the PEGBIS model with the incident offshore height of $(H_{1/3})_0=0.240$ m and $\theta_0=17.3^\circ$. As shown in Fig. 8, the computed wave height agrees well with the measurements. The computation of longshore currents yields good agreement with the measurements when the energy transfer factor from waves to surface rollers is set at $\alpha=0.5$. If the contribution of surface rollers is neglected, the computed result yields the longshore current profile much shifted offshore. Horizontal mixing is calculated with the turbulent eddy viscosity with the constant value of $A=0.05$ and the bottom frictional coefficient of $C_f=0.007$.

Reniers and Battjes (1997) made a laboratory test for a barred beach made of concrete in a wave basin at Delft University of Technology. The incident waves were $H_{rms}=0.07$ m, $T_p=1.2$ s, and $\theta=30^\circ$ in the section of uniform depth of $h=0.55$ m. The values of measurement data were read off on the enlarged copies of relevant diagrams of their paper. The

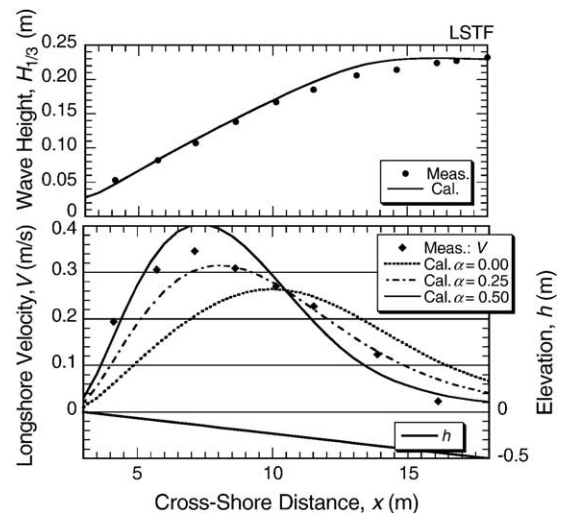


Fig. 8. Comparison of PEGBIS prediction ($A=0.05$ and $C_f=0.007$) and laboratory data by Hamilton and Ebersole (2001) on a uniform concrete slope of $s=1/30$.

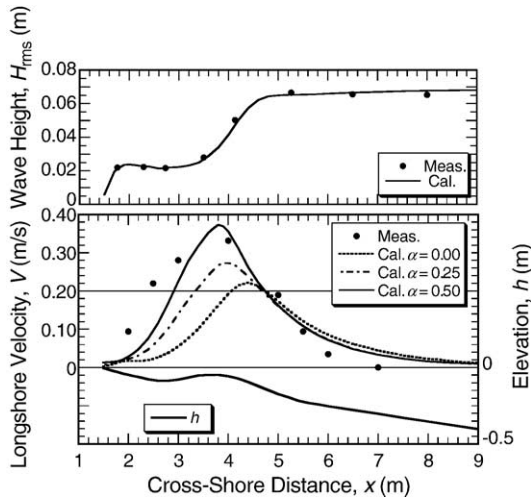


Fig. 9. Comparison of PEGBIS prediction ($A=0.05$ and $C_f=0.025$) and laboratory data by Reniers and Battjes (1997) on a barred concrete beach.

wave height data were shown at five different cross sections, but their means by visual judgment are employed here as representative values. Comparison of computation and measurements is shown in Fig. 9.

The computed wave height agrees well with the measurements. Computation of longshore currents with the surface roller energy transfer factor of $\alpha=0.5$ yields reasonable agreement with the measurements, although the coefficient of bottom friction has to be increased to $C_f=0.025$ from the value of 0.015 used by Reniers and Battjes (1997).

Laboratory tests on movable bed have been reported by Wang et al. (2002), who carried out measurements in the LSTF with the sediment of quartz sand having the median diameter of 0.15 mm. Two tests for spilling breakers and plunging breakers were conducted for detailed measurements of wave height, longshore and cross-shore currents, suspended sediment concentration, and longshore sediment transport rate. Measurements were taken on the quasi-equilibrium beach profiles for

both the spilling and plunging profiles. Wave height and longshore current data and the beach profiles were read off on the enlarged copies of respective diagrams in their paper.

The incident wave conditions were targeted at $H_{1/3}=0.25$ m, $T_p=1.5$ s, and $\theta=10^\circ$ for the spilling breaker case and $H_{1/3}=0.23$ m, $T_p=3.0$ s, and $\theta=10^\circ$ for the plunging breaker case in front of wave generators located at the depth of $h=0.90$ m. The input wave heights for numerical computation were modified to $H_{1/3}=0.27$ m and 0.28 m for spilling and plunging breakers, respectively, so as to reproduce the wave heights in the offshore region as much as possible. Comparisons of PEGBIS predictions with measurements for the spilling and plunging breaker cases are shown in Fig. 10.

Predicted wave heights are in good agreement with the measured ones, although the prediction is slightly lower for the spilling breaker case and slightly higher for the plunging breaker case. The measured longshore current velocities tended to increase toward the shoreline for the both cases. However, numerical computations show a gradual decrease toward the shoreline and cannot reproduce such a tendency. Because the test on a concrete slope in the LSTF did not indicate such a tendency of velocity increase toward the shoreline as shown in Fig. 8, some mechanism characteristic to a movable bed may have been working on the generation of longshore currents there. Except for the region near to the shoreline, the predicted longshore velocity with the surface roller energy transfer factor $\alpha=0.25$ to 0.50 almost agrees with the measurements for the spilling breaker case. The prediction without surface rollers ($\alpha=0$) fails to simulate measurements, again demonstrating the importance of incorporating surface roller effects in the longshore current generation.

7. Comparison of predictions by PEGBIS model and field measurement data

The first systematic field measurements of longshore currents were carried out at Leadbetter Beach, California, in

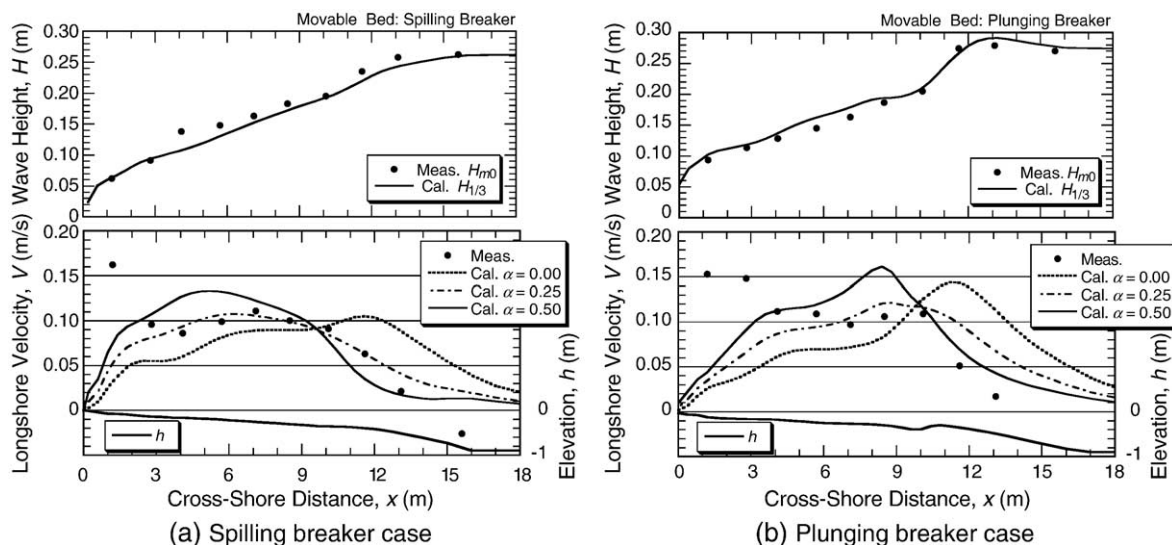


Fig. 10. Comparison of PEGBIS prediction ($A=0.10$ and $C_f=0.020$) and laboratory data by Wang et al. (1997) on movable bed beaches.

February 1980, as reported by Thornton and Guza (1986). Two cases from their paper are used to validate the computation by the PEGBIS model. The beach profiles, wave heights, and longshore current velocities were read off on the enlarged copies of respective diagrams. Comparisons of the predictions and measurements for February 4 and 5 are shown in Fig. 11.

Computation of wave heights by the PEGBIS model was carried out by setting the free parameters $C_b=0.060$ and $C_b^*=0.0525$, which are 25% lower than the standard values of Eqs. (8) and (9) The adjustment was necessary to bring forth good agreement between the prediction and the measurement. The observed waves were typical swell with the steepness of $H_0/L_0 \approx 0.0024$ and waves of such a low steepness may have the breaking limit height much lower than waves of ordinary steepness. Eq. (11) for the breaker index by Battjes and Stive (1985) suggests such a tendency, although such a lowering of breaking limit height was not supported by the field data at Ajigaura Coast (Fig. 17 of Goda 2004). Wave transformation at Leadbetter Beach was carried out by assuming 1-D beach profiles (straight, parallel depth-contours) and by assigning the spectral peak enhancement factor $\gamma=7.0$ for the JONSWAP type spectrum and the directional spreading parameter $s_{max}=200$ for the Mitsuyasu type spreading function in consideration of the very low swell steepness.

The measured wave heights on February 4 are slightly smaller than the calculation, indicating stronger wave dissipation than the model prediction. Nevertheless the computed longshore current velocities fit well with the measurement for a surface energy transfer factor $\alpha=0.25$, rather than $\alpha=0.50$; the same applies for the data of February 5. Because of the very low steepness, plunging type breakers must have been predominant on the days of measurements. If so, formation of surface rollers must have been rather weak, because a majority of wave energy dissipated by breaking must have immediately been consumed in the form of intensive turbulence associated with large vortices. It would be interesting to

investigate how the surface roller energy transfer factor varies with respect to wave characteristics.

Another available field measurement data set on longshore currents are those of DELILAH project carried out at Duck, North Carolina in October 1990. Several papers examining the data have been published. In the present paper, the data of the mid tide of October 11 were read off from the paper by Thornton and Kim (1993) and those at 2200 hours of October 14 from the paper by Smith et al. (1993). The offshore wave conditions were determined from the diagrams in these papers as listed on the caption of Fig. 12. A small adjustment by a trial and error procedure was made to the offshore wave heights to make the computed wave heights outside the surf zone in agreement with the measurement data there. The input wave spectrum on October 11 was assumed to have the peak enhancement factor of $\gamma=3.3$ and the directional spreading parameter of $s_{max}=50$ and that of October 14 as having $\gamma=3.3$ and $s_{max}=100$. These values were subjectively selected on the basis of wave data. The free parameters for wave breaking were set at $C_b=0.070$ and $C_b^*=0.0613$. Fig. 12 shows comparison of the predictions by the PEGBIS model and the measured data. Predicted wave heights agree well with the measurements.

As for the longshore current velocity, numerical computation is carried out with the surf roller energy transfer factor set at $\alpha=0.5$. Two levels of horizontal mixing with the constant values of $A=0.3$ and 0.5 are tried, but there are only small differences. The numerical computations as a whole cannot reproduce the observed cross-shore profiles of longshore currents. For the data of October 11, longshore currents were quite strong in the region beyond the distance 250 m, which was clearly outside the surf zone, and no wave-induced currents could be expected. Longshore currents outside the surf zone were also significant in the data of October 14. Furthermore, the data show the fastest currents occurred around the distance 160 m, which was located in the trough area.

Appearance of strong longshore currents at the trough zone was the characteristic findings of the DELILAH project, and

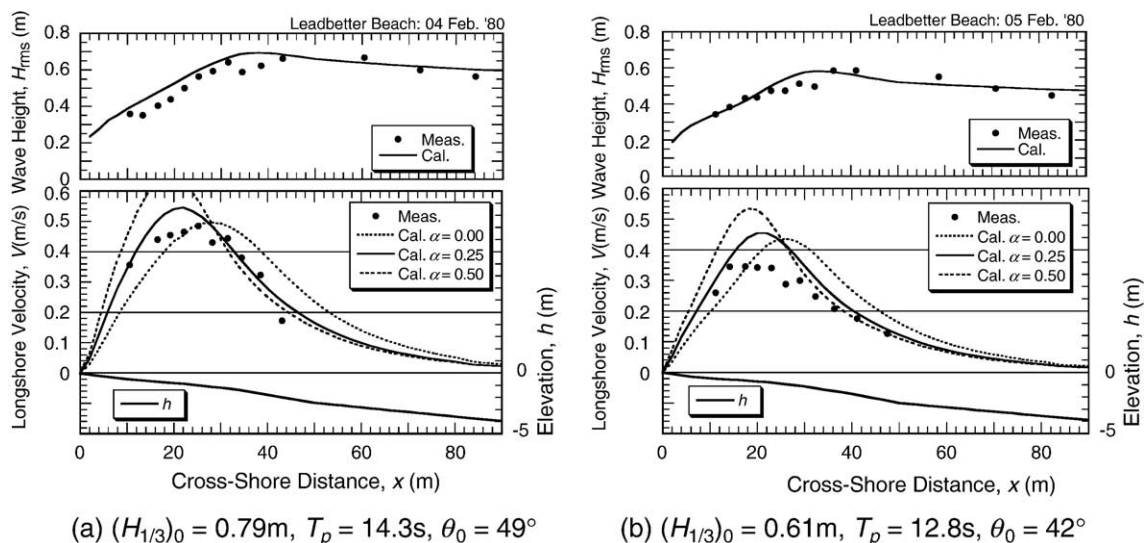


Fig. 11. Comparison of PEGBIS prediction ($A=0.50$ and $C_f=0.007$) and Leadbetter Beach data by Thornton and Guza (1986).

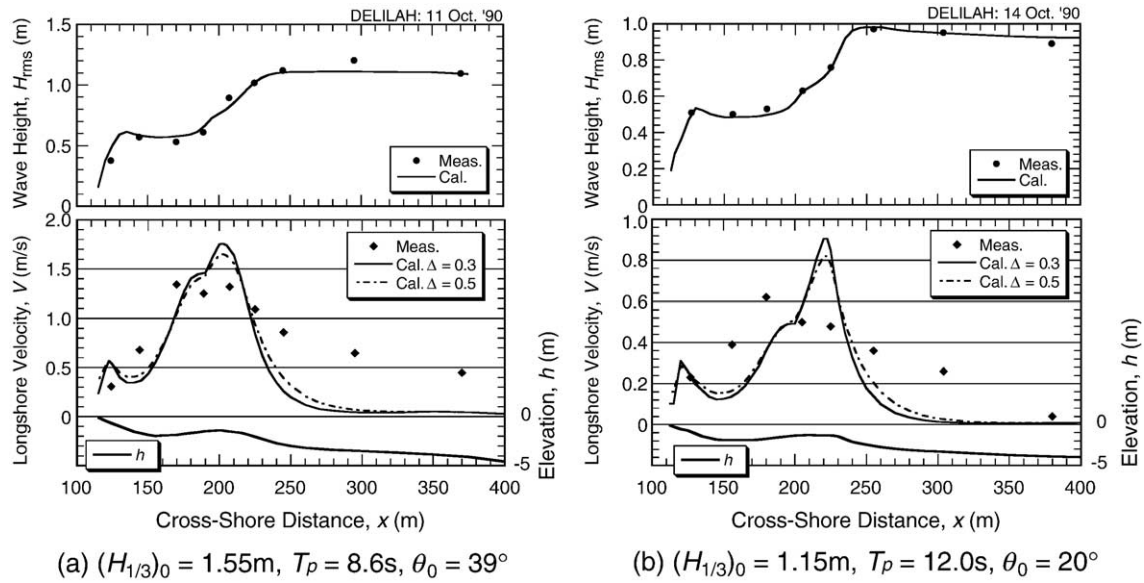


Fig. 12. Comparison of PEGBIS prediction ($\alpha=0.50$ and $C_r=0.0075$) and the data from DELILAH Project by Thornton and Kim (1993) and Smith et al. (1993).

various efforts have been made to explain the phenomenon. Smith et al. (1993) introduced the turbulent kinetic energy transport equation, but obtained only a slight improvement for velocity increase at the trough area. Reniers et al. (1995) examined the data of October 10 for alongshore variation of the mean water level, which was caused by alongshore non-uniformities of beach profiles. They concluded that the mean water level variation produced alongshore pressure gradients and they contributed to the increase in the longshore currents in the trough area.

Further comparison of the numerical predictions and field measurements is made for the data along a pier called the Hazaki Oceanographical Research Station (HORS) of the Port at Harbour Research Institute, located at Hazaki Coast in Ibaraki Prefecture, Japan, as reported and analyzed by Kuriyama and Ozaki (1993, 1996). The data of beach profiles,

wave heights, and longshore currents were kindly provided by Dr. Yoshiaki Kuriyama. The beach profiles around HORS had a certain alongshore variation, but the mean profile averaged over the alongshore width of 60 m around the pier is used in the present analysis. Fig. 13 shows the comparison of PEGBIS predictions and measurements. The offshore wave conditions are listed on the caption of Fig. 13. A small adjustment to the offshore wave heights has been made as before. Wave transformation was calculated with the free parameters for wave breaking being set at $C_b=0.060$ and $C_b^2=0.0525$. The computed wave heights are slightly lower in the outer half of the surf zone and higher in the inner half than the measured heights, but as a whole the computations and measurements are in agreement.

Patterns of the cross-shore variation of longshore currents observed at HORS are well reproduced by the numerical

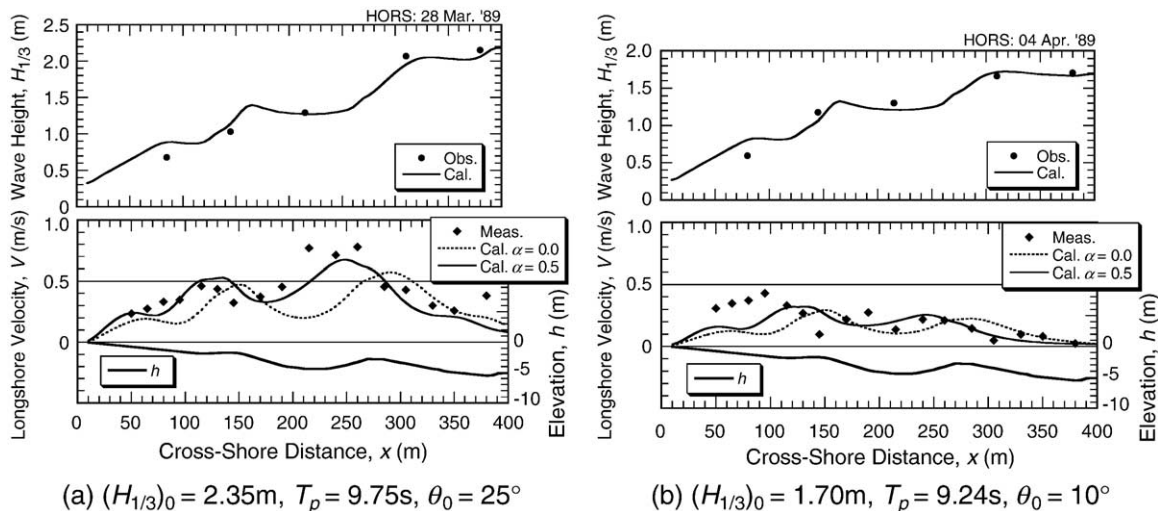


Fig. 13. Comparison of PEGBIS prediction ($A=1.0$ and $C_r=0.0075$) and the data taken at HORS by Kuriyama and Ozaki (1993).

computation when the surface roller effect is introduced with the energy transfer factor of $\alpha=0.5$. The result is another confirmation for the necessity of incorporating the surface rollers in the longshore current computations. However, there are some differences between the measurements and the prediction. Strong currents observed around the distance 380 m on March 28 and those around the distance 80 m on April 4 cannot be explained by the current driving force by waves. There must have been some other driving forces such as winds, ambient currents, etc.

Both the sites of Duck and Hazaki are located on the open coast where waves are incident from all directions. On the other hand, Leadbetter Beach is located at a restricted coast sheltered by the Channel Islands in the southwest and the Point Conception in the northwest, and thereby the wave approach is limited within a narrow window ($\pm 9^\circ$ centered on 249°). In the case of Leadbetter Beach, the longshore velocity predictions agree well with measurements as shown in Fig. 11, while in the cases of Duck and Hazaki Coasts the agreement was only fair. At Leadbetter Beach, the current driving force of waves probably surpassed other driving forces such as winds, ambient currents, etc. and the situation was rather similar to laboratory test conditions.

8. Discussion on empirical constant values

Numerical models for wave transformation by breaking and longshore currents induced by them employ several empirical constants. In the PEGBIS model, the breaking limit constant C_b is the main parameter governing the heights of breaking waves. In the longshore current computation, the energy transfer factor α from waves to surface rollers, a constant A for the turbulent eddy viscosity by Larson and Kraus formula, and the coefficient of bottom friction C_f affect the speed and cross-shore distribution of longshore currents. In the present paper, no optimization of these empirical constants has been attempted, because there are so many parameters involved. Values of these empirical constants were selected to provide acceptable agreement between the computations and measurements based on the author's subjective judgment. Nevertheless, a list of the constant values will provide the readers some guidelines for applications of the numerical model; see Table 2.

The breaking limit constant C_b was varied from 0.06 to 0.08 to obtain good agreement with the measured wave heights. A fine-tuning of wave height is necessary in

longshore current computation, because only a small change in wave height curves yields a large difference in longshore current velocities.

The surface roller energy transfer factor can be taken at $\alpha=0.5$ for most cases, but the cases of swell with very low steepness at Leadbetter Beach clearly favored the value $\alpha=0.25$. The empirical constant for the turbulent eddy viscosity formula by Larson and Kraus (1991) tends to be small for laboratory conditions and large for field data: the former in the range of 0.05 to 0.10, while the latter in the range of 0.5 to 1.0. It seems to reflect the difference in the magnitude of turbulence between laboratory and field conditions.

The fitted values of the bottom friction coefficient C_f varied from 0.0070 to 0.0250 for laboratory tests, while they were 0.007 to 0.0075 for the field data. The reason for a large coefficient value for some of laboratory tests has not been clarified. Further validation data is needed for clarification.

9. Conclusions

- 1) Currently available models for wave transformation by random breaking produce large differences on wave heights in the surf zone and longshore current velocities induced by random waves. Any wave model for longshore current applications should be scrutinized for its predictive capacity through validation with as many laboratory and field measurement data sets as possible.
- 2) The formulation of the turbulent eddy viscosity by Larson and Kraus (1991) for horizontal mixing process functions nearly the same as that by Battjes (1975). Because of its simple functional form, it can be useful for practical applications.
- 3) Incorporation of the surface roller term in the longshore current equation is vital for reliable prediction of longshore current velocities induced by random waves. An energy transfer equation from the wave energy dissipated by breaking to the surface roller energy facilitates the computation process.
- 4) The surface roller energy transfer factor is 0.5 at most, but it seems less for swell of very low steepness that breaks in plunging form.
- 5) The PEGBIS (*Parabolic Equation with Gradational Breaker Index for Spectral wave*) wave transformation model by Goda (2004) has been verified to have the capability of predicting wave height variations and longshore current velocities in the surf zone on beaches with straight, parallel depth contours, as the result of comparisons with four laboratory test cases and three field data sets.
- 6) On the open coast, various current driving forces other than waves seem to be working on generating longshore currents. Thus, prediction by a wave model alone may not yield complete agreement with field measurements.

Acknowledgements

The author wishes to express his sincere thanks to Professors J. A. Battjes and E. B. Thornton for their critical

Table 2
List of empirical constant values employed in the present paper

Type	Test cond./Location	C_b	α	A	C_f
Laboratory	Uniform slope (fixed bed)	0.08	0.5	0.05	0.0070
	Barred beach (fixed bed)	0.08	0.5	0.05	0.0250
	Spilling breakers	0.08	0.25–0.5	0.10	0.0200
	Plunging breakers	0.07	0.25–0.5	0.10	0.0200
Field	Leadbetter beach	0.06	0.25	0.5	0.0070
	DELILAH	0.07	0.5	0.5	0.0075
	HORS	0.06	0.5	1.0	0.0075

reviews with thoughtful comments, which helped to improve the clarity of the paper.

References

- Baldock, T.E., Holmes, P., Bunker, S., Van Weert, P., 1998. Cross-shore hydrodynamics within an unsaturated surf zone. *Coast. Eng.* 34 (3-4), 173–196. (Discussions by Y. Goda and the authors' reply in *Coastal Engineering*, 36 (2), pp. 165–166).
- Battjes, J.A., 1972. Setup due to irregular wave. *Proc. 13th Int. Conf. Coastal Eng.* ASCE, Vancouver, pp. 1993–2004.
- Battjes, J.A., 1974. Computation of Set-Up, Longshore Currents, Run-Up and Overtopping Due to Wind-Generated Waves. Dept. Civil Eng., Delft Univ. of Technology, Report, vol. 74-2. 244 pp.
- Battjes, J.A., 1975. Modeling of turbulence in the surf zone. *Proc. Symp. Modeling Techniques*, pp. 1050–1061.
- Battjes, J.A., Janssen, J.P.F.M., 1978. Energy loss and set-up due to breaking of random waves. *Proc. 16th Int. Conf. Coastal Eng. ASCE, Hamburg*, pp. 1–19.
- Battjes, J.A., Stive, M.J.F., 1985. Calibration and verification of a dissipation model for random breaking waves. *J. Geophys. Res.* 90 (C5), 9159–9167.
- Collins, J.I., 1970. Probabilities of breaking wave characteristics. *Proc. 12th Int. Coastal Eng. Conf. ASCE, Washington, D.C.*, pp. 399–414.
- Dally, W.R., Brown, C.A., 1995. A modeling investigation of the breaking wave roller with application to cross-shore currents. *J. Geophys. Res.* 100 (C12), 24873–24883.
- Dally, W.R., Dean, R.G., Darlymple, R.A., 1985. Wave height variation across beaches of arbitrary profile. *J. Geophys. Res.* 90 (C6), 11,917–11,927.
- Goda, Y., 1975. Irregular wave deformation in the surf zone. *Coast. Eng. Jpn.* 18, 13–26 (JSCE).
- Goda, Y., 2000. *Random Seas and Design of Maritime Structures*, 2nd ed. World Scientific, Singapore.
- Goda, Y., 2004. A 2-D random wave transformation model with gradational breaker index. *Coast. Eng. J.* 46 (1), 1–38 (JSCE and World Scientific).
- Goda, Y., Watanabe, Y., 1991. A longshore current formula for random breaking waves. *Coast. Eng. Jpn.* 34 (2), 159–175 (JSCE).
- Hamilton, D.G., Ebersole, B.A., 2001. Establishing uniform longshore currents in a large-scale sediment transport facility. *Coast. Eng.* 42, 199–218.
- Hirakuchi, H., Maruyama, K., 1986. An extension of the parabolic equation for application to obliquely incident waves. *Proc. 33th Japanese Conf. Coastal Engng.* pp. 114–118 (in Japanese).
- Kuo, C.T., Kuo, S.T., 1974. Effect of wave breaking on statistical distribution of wave heights. *Proc. Civil Eng. Ocean*, 1211–1231 (ASCE).
- Kuriyama, Y., Ozaki, Y., 1993. Longshore current distribution on a bar-trough beach-field measurements at HORS. *Rep. Port Harb. Res. Inst.* 32 (3), 3–37.
- Kuriyama, Y., Ozaki, Y., 1996. Wave height and fraction of breaking waves on a bar-trough beach-field measurements at HORS and modeling. *Rep. Port Harb. Res. Inst.* 35 (1), 1–38.
- Larson, M., Kraus, N.C., 1991. Numerical model of longshore current for bar and trough beaches. *J. Waterw. Port Coast. Ocean Eng.* 117 (4), 326–347 (ASCE).
- Longuet-Higgins, M.S., 1970. Longshore current generated by obliquely incident sea waves, 1 & 2. *J. Geophys. Res.* 75 (33), 6779–6801.
- Reniers, A.J.H.M., Battjes, J.A., 1997. A laboratory study of longshore currents over barred and non-barred beaches. *Coast. Eng.* 30, 1–22.
- Reniers, A.J.H.M., Thornton, E.B., Lippmann, T.C., 1995. Longshore currents over barred beaches. *Proc. Coastal Dynamics '95*, pp. 413–424.
- Ruessink, B.G., Miles, J.R., Feddersen, F., Guza, R.T., Elgar, S., 2001. Modeling the alongshore current on barred beaches. *J. Geophys. Res.* 106 (C10), 22451–22463.
- Smith, J.McK., 2001. Breaking in a spectral wave model. *Ocean Wave Measurement and Analysis (Proc. WAVES 2001)*. ASCE, pp. 1022–1031.
- Smith, J.McK., Svendsen, I.A., Putrevu, U., 1992. Vertical structure of the nearshore current at DELILAH: Measured and modeled. *Proc. 23rd Int. Conf. Coastal Eng. ASCE, Venetia*, pp. 2825–2838.
- Smith, J.McK., Larson, M., Kraus, N.C., 1993. Longshore current on a barred beach: Field measurement and calculation. *J. Geophys. Res.* 98 (C12), 22717–22731.
- Svendsen, I.A., 1984a. Wave heights and set-up in a surf zone. *Coast. Eng.* 8, 303–329.
- Svendsen, I.A., 1984b. Mass flux and undertow in a surf zone. *Coast. Eng.* 8, 347–365.
- Tajima, Y., Madsen, O.S., 2002. Shoaling, breaking and broken wave characteristics. *Coastal Engineering 2002, Proc. 28th Int. Conf. World Scientific, Cardiff, Wales*, pp. 222–234.
- Tajima, Y., Madsen, O.S., 2003. Modeling near-shore waves and surface roller. *Proc. 2nd Int. Conf. Asian and Pacific Coasts (APAC 2003)*, Makuhari, Chiba, Japan, Paper no. 28 in CD-ROM, 12 pp.
- Thornton, E.B., Guza, R.T., 1983. Transformation of wave height distribution. *J. Geophys. Res.* 88 (C10), 5925–5938.
- Thornton, E.B., Guza, R.T., 1986. Surf zone longshore currents and random waves: field data and models. *J. Phys. Oceanogr.* 16, 1165–1178.
- Thornton, E.B., Kim, C.S., 1993. Longshore currents and wave height modulation at tidal frequency inside the surf zone. *J. Geophys. Res.* 98, 16509–16519.
- Wang, P., Ebersole, B.A., Smithe, R., Johnson, B.D., 2002. Temporal and spatial variations of surf-zone currents and suspended sediment concentration. *Coast. Eng.* 46, 175–211.